

# Mechanical and Tribological Behaviour of ADC12 alloy reinforced by Nano- $\text{Al}_2\text{O}_3$ Particles with Addition of Al-Sr and Al-5Ti-B Produced by Stir Casting Method

AJRI



Author Notification  
27 August 2019  
Final Revised  
28 August 2019  
Published  
03 September 2019

Muhammad Wira Akira<sup>1</sup>, Hanuna Haritsah<sup>2</sup>, Anne Zulfia<sup>\*3</sup>, Ekavianti Prajateljia<sup>4</sup>  
Institut Teknologi Bandung<sup>1,4</sup> Universitas Indonesia<sup>2,3</sup>  
e-mail: [akirawira@gmail.com](mailto:akirawira@gmail.com), [hanunaharitsah@gmail.com](mailto:hanunaharitsah@gmail.com), [anne@metal.ui.ac.id](mailto:anne@metal.ui.ac.id),  
[ekaprajateljia@gmail.com](mailto:ekaprajateljia@gmail.com)

\*corresponding author

To cite this document : Muhammad Wira Akira, Haritsah, H., Anne Zulfia, & Prajateljia, E. (2021). Mechanical and tribological properties of nano-sized  $\text{Al}_2\text{O}_3$  particles on ADC12 alloy composites with Strontium modifier produced by stir casting method. *ADI Journal on Recent Innovation*, 3(1), 9–20.

DOI : <https://doi.org/10.34306/ajri.v3i1.346>

Hash :  
ABCqoayvX42Vnn5WMXKk3g77jAvTr58WfVWsAE5ZKmDOW1kyZF0KSok7ehGBG3cJ

## Abstract

*Nano- $\text{Al}_2\text{O}_3$  particles were incorporated into ADC12 alloy with the addition of Al-5Ti-B, Al-Sr, and Mg to achieve high performance in mechanical and tribological properties. In this study, varied nano- $\text{Al}_2\text{O}_3$  was used from 0.25 vf-% to 0.5 vf-% through stir casting methods to discover the optimum amount to obtain high performance. Besides, the inclusion of grain refiner Al-5Ti-B and microstructure modifier Al-Sr is expected to improve performance to the next level. However, porosity and agglomeration still be a concern in Aluminum alloy matrix composite fabrication. The presence of spinel phase  $\text{MgAl}_2\text{O}_4$  in the interface area between nano- $\text{Al}_2\text{O}_3$  particles and ADC12 alloy is relied upon to minimize this porosity and agglomeration issue. The optimum of tensile strength and hardness was found at 0.35 vf-%  $\text{Al}_2\text{O}_3$  and wear rate at 0.4 vf%. Although, the optimum point of wear found at 0.4 vf%, porosity began to increase at 0.4 vf% as well. As a result, 0.35 vf% addition of the nano- $\text{Al}_2\text{O}_3$  gives the best performance for the composite.*

*Keywords: aluminium matrix composite, ADC12 alloy, nano- $\text{Al}_2\text{O}_3$  particles, stir casting, strontium modifier.*

## I. INTRODUCTION

Aluminum Matrix Composites (AMCs) with excellent physical and mechanical properties are increasingly in demand for high-performance applications such as automotive, military, aerospace, and electricity industries. The excellence of Aluminum matrix composites (AMCs) compared to the conventional Al and its alloys are preferable since they have a higher strength-to-weight ratio, stiffness-to-weight ratio, wear resistance, creep resistance and thermal durability [1, 2].

Presently, nano-sized ceramic particle reinforcements were developed in metal matrix composites and proven that the effect of decreasing size of ceramic particle reinforcements is distinctly improved the mechanical properties [3]. Sajjadi et al. on their work, revealed that reducing reinforcement particle size in aluminum composite affect the increase of hardness and compressive strength remarkably, which make them attractive for numerous industrial applications. The Al–Si–Cu alloy ADC12 was chosen as a matrix due to its excellent material properties, namely high cast-ability, low density, high productivity, low shrinkage rate, and relatively high strength. Equally important, nano-sized  $\text{Al}_2\text{O}_3$  particle was employed as inert ceramic reinforcement, which has high specific stiffness, superior high temperature, and excellent mechanical properties [1, 4, 5].

The mechanical properties of composites are not only influenced by reinforcing particles but also grain size, secondary dendrite arm spacing (SDAS) and the size and morphology of the eutectic silicon structures formed, as well as the type of defects that emerge [6]. The microstructure of silicon crystal hypoeutectic Al-Si as cast (ADC12) whose morphology is relatively rough and needles or beams form can produce parts that have a higher stress level provided that lessen its strength and toughness [7].

However, the development of nano-sized particle reinforcements remains challenges. A few studies reported the existence of agglomeration and high porosity being the biggest challenges in nano-sized AMCs [4]. The agglomeration phenomenon occurs due to the increase of energy on the surface between reinforcement and matrix, therefore causing poor wettability at the interface and ununiform nano-particle distribution. Ununiform distribution can lead to differences hardness in some areas [8]. As the most critical aspect of adhesion in metal matrix composites, wettability is measured by contact angle  $\theta$  which depends on the surface energy of solid/liquid  $\gamma_{SL}$ , liquid/vapour  $\gamma_{LV}$ , and solid/vapour  $\gamma_{SV}$  according to Young's equation 1.

$$\cos\theta = \frac{\gamma_{SA} - \gamma_{LS}}{\gamma_{LA}} \quad (1)$$

Good wettability can be achieved if the contact angle has a tendency  $\theta < 90^\circ$ . In the previous study,  $\text{Al}_2\text{O}_3$  wettability has been investigated by sessile drop method, which shows that  $\text{Al}_2\text{O}_3$  particles have a poor wettability on molten aluminum [9]. In research conducted by Ali et al. contact angle  $\theta < 90^\circ$  of  $\text{Al}_2\text{O}_3/\text{Al}$  composite will achieve by the addition of 5 wt% reactive elements Magnesium for 400 seconds. Wettability is affected by the reaction between magnesium and alumina at the metal-oxide interface to form  $\text{MgAl}_2\text{O}_4$ , where this phase can break the oxide layer on the surface of the molten aluminum, as a result, a wettability enhanced [10].

Herein, the merits of Al-5Ti-B as a grain refiner and Al-Sr as a modifier agent will lead to remarkable enhanced mechanical properties of nano-size AMCs. Reduced grain size will affect strength and material resistance to deformation. It is caused by dislocation pile-up around the grain boundary then accumulated to produce a large dislocation density [11]. The investigation of grain refiner effect on Al-Si alloy by Garcia et al. has proved that Al–5Ti–1B master alloys are suitable grain refining agents for the Al-Si – ceramic particles composites leading to the more uniform distribution of reinforcements particles. They revealed more amount of Ti-B gives a smaller grain size. In this case, Al–5Ti–1B ternary master alloy with 0.15 wt% Ti and 0.03 wt% B composition shows the optimum result with fine equiaxed grains with the average 450  $\mu\text{m}$  in diameter [12]. Correspondingly, the modifying agent was added that aims that improve the mechanical properties by altering the structure of the eutectic silicon. Saeed et al. have discovered the addition of 0.4% Al-Sr on ADC12 alloy change

sharp-rough Al-Si eutectic phase turn into fibrous and enhanced tensile strength of its alloy [13].

Fabrication of nano-size AMCs was performed by stir casting method, which relatively simple and low-cost process. Gowrishankar et al. observed that stir casting is an effective method for manufacturing aluminum composites. It shows better matrix-particle bonding- due to the formation of a vortex while during stirring action of particles into the melts. Thus a uniform distribution of reinforcements and hardness on the entire cross-section was achieved [14]. This study will examine the ideal volume fraction of nano-size  $\text{Al}_2\text{O}_3$  on ADC12 composite with the addition of modifier agent Al-Sr along with grain refiner Al-5Ti-B on its mechanical and tribological properties.

## II. METHODE

### Material Preparation

ADC12 aluminum alloy was used as matrix composites that have chemical composition given in Table I.

Si	Cu	Mg	Fe	Ni	Mn	Zn	Al
10.5	2.33	0.21	0.86	0.08	0.23	0.64	Res t

Table I. Chemical Composition of ADC12 Alloy

Nano- $\text{Al}_2\text{O}_3$  particles prepared as reinforcements was given in varies of volume fraction; 0.25 vf%; 0.3 vf%; 0.35 vf%; 0.4 vf%; 0.5 vf%. Wetting agent Mg, grain refiner master alloy Al-5Ti-B ingot, and modifier agent Al-Sr also used into the composite a number of 5 wt%, 0.15 wt%, and 0.04 wt% respectively. Nano- $\text{Al}_2\text{O}_3$  particles have a range of particle sizes 27 – 35 nm with nearly spherical morphology as shown in figure 1. Nano- $\text{Al}_2\text{O}_3$  particles were prepared by mixing with 3% stearic acid ( $\text{C}_{18}\text{H}_{36}\text{O}_2$ ) for a certain time. Subsequently, the mixture was diluted in alcohol using ultrasonic vibrator for 6 minutes. The solution contains nano- $\text{Al}_2\text{O}_3$ , stearic acid ( $\text{C}_{18}\text{H}_{36}\text{O}_2$ ), and alcohol ( $\text{C}_2\text{H}_5\text{OH}$ ) was heated in a muffle furnace at  $1000^\circ\text{C}$  for 1 hour to evaporate alcohol content. Your paper must be in two column format with a space of 8.5mm (0.34") between columns.

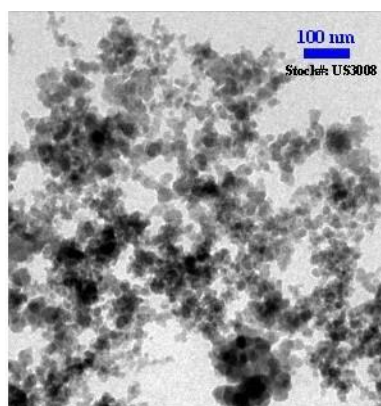


Figure 1. SEM image of nano- $\text{Al}_2\text{O}_3$  particles size.

### Composite Fabrication

Initially, the temperature of tilting crucible furnace was heated gradually to 800°C for melting process then the ADC12 ingot was placed into a furnace with an appropriate amount. At the same time, mould and stirrer were coated with a mixture of zirconia powder and thinner to easily the casting product to be removed. The mould was preheated at 400°C to avoid thermal shock and also evaporate the moisture content. After the aluminum was melted, slag at the surface of molten metal was skimmed and immediately purged argon to molten for 2 minutes. After that, 5 wt% Mg ingot, 0.15 wt% Al-Ti-B ingot, and 0.04 wt% Al-Sr were added sequentially. The molten mixture was stirred for 2 minutes at a rate of 600 rpm followed by addition of nano- $\text{Al}_2\text{O}_3$  particles. Then the degassing process is carried out again for a minute. In a moment, the molten mixture was poured into the mould followed by cooling down at room temperature at a certain time.

### Characterization

Metallography investigation was conducted using ASTM standard E3 – 11. Samples were prepared by the ground the surface through #800 to #1500 using sandpaper and polished using  $\text{TiO}_2$  paste on velvet fabric. The etching was performed using Keller's reagent. Microstructural was observed by Optical Microscopy (OM, Zeiss Primotech). The elements were also investigated using Optical Emission Microscope (OES, Spectro APL 3460), Energy Dispersive Scanning which equipped form SEM (SEM, JEOL JSM-6360 LA) and X-Ray Diffraction (XRD, Shimadzu XRD-70 10). The interface between matrix and reinforcements investigation was conducted using SEM (Scanning Electron Microscopy). Tensile tests were performed based on ASTM: B557M – 02 (UTM Gottech AL-7000 LA). Hardness tests were performed using Rockwell B method based on ASTM E18-11 (Rocky model). Wear tests were performed with parameter:- the sliding distance at 400 mm, load 3.16 kgf, and speed 1.97 m/s (Ogoshi model). The experimental density of the composites was measured by the Archimedes principle. Density tests by the law of Archimedes were carried out to determine the density of a sample.

## III. RESULT AND DISCUSSION

### Mechanical properties of ADC12 nano- $\text{Al}_2\text{O}_3$ composites

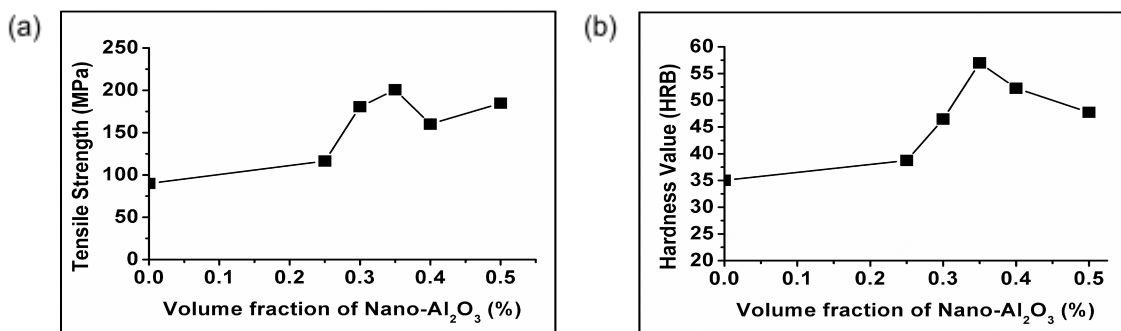


Figure 2. Effect of nano- $\text{Al}_2\text{O}_3$  volume fraction addition on (a) tensile strength and (b) hardness properties

Figure 2a shows tensile strength increase gradually with an increasing volume fraction of nano- $\text{Al}_2\text{O}_3$  particles from ADC12 alloy up to 0.35 vf% then decrease besides of 0.4vf% to 0.5vf%. Figure 2b shows hardness value which has an identical trend with tensile strength graph. Hardness increase with the addition of volume fraction of nano- $\text{Al}_2\text{O}_3$  up to 0.35 vf% then began to decrease besides 0.4 vf% to 0.5vf%.

Increasing the volume fraction of nano- $\text{Al}_2\text{O}_3$  particles will increase the dislocation pile-up, thus increasing the tensile strength of the composite. As the volume of nano  $\text{Al}_2\text{O}_3$  fraction

increases, the load transfer from the matrix to reinforcement is getting better. However, tensile strength reduces if the reinforced particle volume fraction is given excess,-; it forms porosity and agglomeration due to the uneven distribution of particles. The difference in thermal expansion between the aluminum matrix and the Nano- $\text{Al}_2\text{O}_3$  particles results in debonding at the interface and decreases the tensile strength of the composite. The addition of magnesium can reduce the surface tension with the presence of  $\text{MgAl}_2\text{O}_4$  spinel phase which acts as interfaces that shows the ability to increase the strength of the matrix to make the load can transfer more effective [15]. Furthermore,  $\text{Mg}_2\text{Si}$  intermetallic phase which has high melting point, low density, high hardness, and high elastic modulus, also has a role as a reinforcing mechanism as a dislocation barrier on the ADC12 alloy matrix [16].

### Tribological properties of ADC12 nano- $\text{Al}_2\text{O}_3$ composites

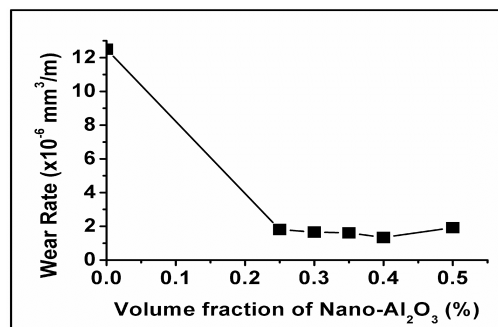


Figure 3. Effect of volume fraction nano- $\text{Al}_2\text{O}_3$  addition on the wear rate of ADC12 /  $\text{Al}_2\text{O}_3$  composite

The results of the wear rate test are shown in figure 3. ADC12 alloy has wear rate at  $1.25 \times 10^{-5} \text{ mm}^3/\text{m}$ , is decreased significantly with the addition of nano  $\text{Al}_2\text{O}_3$  particles up to 0.5vf%. Nano- $\text{Al}_2\text{O}_3$  particles act as reinforcement to increase wear resistance and hardness of composite materials with some mechanisms such as orowan strengthening, grain-refined strengthening, and dislocation strengthening [17]. Besides, silicon in the ADC12 matrix content can increase wear resistance. Through the solidification process,  $\alpha\text{-Al}$  emerges in dendrites form and silicon form into 3 phase-: primary, binary, and ternary. First silicon acts as a load-bearing phase during wear so that it will increase wear resistance in the material [18]. The lowest wear rate achieved at 0.4 vf%. Moreover, on the subsequent addition at 0.5 vf%, wear rate is increased due to agglomeration and porosity.

### The porosity of ADC12 nano- $\text{Al}_2\text{O}_3$ composites

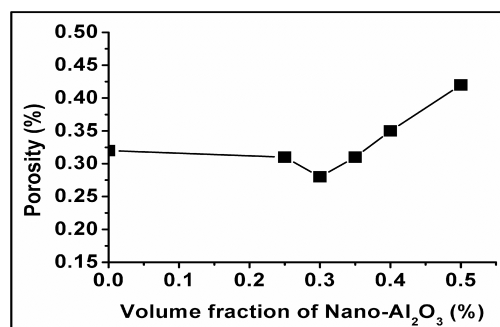


Figure 4. Effect of volume fraction nano- $\text{Al}_2\text{O}_3$  addition on % porosity of ADC12 /  $\text{Al}_2\text{O}_3$  composite

The presence of porosity did not differ significantly between ADC12 alloys with ADC12 / nano- $\text{Al}_2\text{O}_3$  composites with the addition of 0.25 vf% to 0.35 vf% nano- $\text{Al}_2\text{O}_3$  particles, while significant porosity increases began with the addition of nano- $\text{Al}_2\text{O}_3$  of 0.4% to 0.5% as shown in figure 4.  $\text{MgAl}_2\text{O}_4$  phase was able to cover all nanoparticles up to 0.35 vf%. While on the addition up to 0.4 vf%,  $\text{MgAl}_2\text{O}_4$  phase unable to cover  $\text{Al}_2\text{O}_3$  nanoparticles hence nanoparticles that are not covered by the spinel phase, have low wettability and produce a small gap in the interface. Gap between the particles was arising further as a result of low wettability which tends the particle to agglomerate.

### Fractography analysis

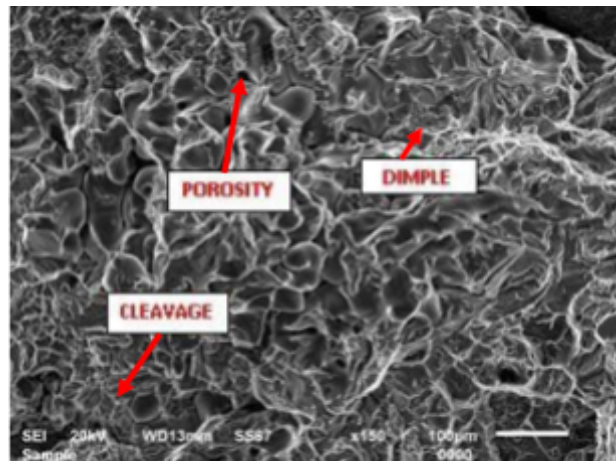


Figure 5 SEM images of 0.35 vf% Nano- $\text{Al}_2\text{O}_3$  on ADC12 / Nano- $\text{Al}_2\text{O}_3$  Composite Fracture Surface

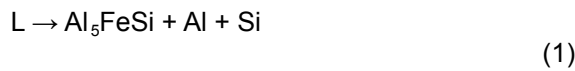
The results of ADC12 / Nano- $\text{Al}_2\text{O}_3$  composite fractography observations with 0.35 vf% nano- $\text{Al}_2\text{O}_3$  particle employed by SEM characterization 150x magnification are shown in Figure 5. It can be seen that there is a mixed type of fracture, namely irregular large dimples and cleavage, which is called Quasi-brittle fracture. Quasi-brittle fracture often occurs in materials, especially in composite materials. The main characteristic of this type of fracture is the combination of 2 types of fractures, namely dimples and cleavage which describe ductile and brittle fractures respectively.

This type of fracture that occurs is also controlled by the addition of the element Sr, which is useful as a modifying agent for  $\text{Mg}_2\text{Si}$  primaries and binaries. Binary  $\text{Mg}_2\text{Si}$  will change to be more globular and fibrous while for primary  $\text{Mg}_2\text{Si}$  there is a change from irregular to more compact [19] which will increase the ductility properties of the composite so that it can compensate for the resulting hardness due to the addition of reinforcing elements. Though the combination of ductility and hardness, the resulting material has good toughness. Typically, the presence of dimples on the fracturing surface is induced by the release of the bonds between the matrix and the reinforcing particle. The fracture occurs along the grain boundary so that it does not cut the grains or particles so that it shows the fracture surface that juts in as if it forms a basin.

From this figure, it can also be seen that there is porosity on the fracture surface. The work by Sajjadi et al. explained the behavior of increased porosity corresponding with the addition of  $\text{Al}_2\text{O}_3$  particles in the aluminum matrix composite [20]. Inadequate interface wetting and particle agglomeration at higher volume fractions are noteworthy considerations for the formation of porosity in composite materials. Therefore, porosity is avoided in AMC composite materials.

### Microstructure analysis

Figure 6a shows ADC12 alloy microstructure without the addition of Al-Sr, Al-5Ti-B, and Mg, observed  $\alpha$ -Aluminum presented in white background phase and silicon eutectic shown in sharp-rough net-like dark gray phase are emerged as the main phase due to 10.5 wt% silicon elements contents. Along with those, other phases also have seen such  $Al_5FeSi$  and  $Al_2Cu$  in needle-like and small gray plate morphology respectively. This phase is typical of the ADC12 alloy because the ADC12 alloy has 0.86 wt.% Fe and 2.33 wt.% Cu content respectively. Therefore, according to the Al-Si-Fe phase ternary system, solidification reaction that occurs as follows : [21]



The addition of 5% magnesium was derived ADC12 alloy ternary system from Al-Si-Cu into Al-Si-Mg. As a result, the intermetallic compound of  $Mg_2Si$  was emerged and formed in primary, binary, and ternary structure during as cast, as shown in figure 6b-f, which lead to improve mechanical properties [19, 22]. This seems to be associated with quasi-binary Al- $Mg_2Si$  derived from the Al-Mg-Si ternary diagram [23].



The number of phases of  $Mg_2Si$  would be directly proportional to the addition of magnesium itself. Due to its characteristics such as low density, high melting point, hardness, and modulus of elasticity,  $Mg_2Si$  intermetallic compounds are one of the important strengthening mechanisms to improve the mechanical properties of these alloys. This intermetallic compound acts as a barrier to the movement of dislocations, thereby contributing to increasing the value of tensile strength. Fine and evenly distributed microstructure  $Mg_2Si$  hinders the movement of dislocations efficiently. However, the emergence of intermetallic compounds also has its drawbacks, the intermetallic compounds in the alloy can also increase porosity [24]. Sharp-rough net-like Al- $Mg_2Si$  eutectic phase in dark gray color spread on the  $\alpha$ -Al matrix, shown in figure 6a, changes into finer and more fibrous after addition of 0.04% Al-Sr, shown figure 6b-f. Research was performed by M. Tebib et al., on the shape transition of the eutectic binary  $Mg_2Si$  defined that the addition of 0.04 wt. % Sr element resulted in a modification of eutectic  $Mg_2Si$  that could be seen from the shifts in the closer distance between their net-like branches shape [25]. The decrease in the distance between these lines can be due to the influence of the amount of undercooling that occurs when a material is combined with strontium.

Strontium critically reduces the eutectic temperature or temperature growth ( $T_g$ ) of the molten alloy. Higher undercooling occur along with a decline in  $T_g$ , which allows the phase generated to be comparatively finer. This morphology phase is closely related to the lower  $r^*$  ( $r$  critical) value, according to equation 2

$$r^* = \frac{2\sigma}{\Delta G_r} = \frac{2\sigma x T_m}{L_m x \Delta T} \quad (2)$$

Where  $r^*$  is the critical nucleus radius,  $\sigma$  is the interfacial energy per unit area,  $T_m$  is the temperature starting to crystallize,  $L_m$  is the latent heat and  $\Delta T$  is the amount of undercooling that occurs. Subsequently, when undercooling is high, it allows the  $r^*$  value to be smaller and increases the possibility of the nucleus forming and consequently the  $Mg_2Si$  produced in the matrix is more abundant and finer [26]. The refinement and modification process only occurs in composite materials with an elemental content of 0.04 wt% Sr. Another mechanism is the low solubility of strontium in magnesium, which induces a lot of strontium to segregate in front

of the growing interface of the eutectic binary  $Mg_2Si$  phase to impede the growth process of the eutectic binary  $Mg_2Si$  itself.  
Grain size also decreases with the addition of Al-5Ti-B and nano- $Al_2O_3$  as seen in figure 6f compare with ADC12 alloy in figure 6a. Nano- $Al_2O_3$  not only serves as an obstacle for dislocation but also the place where the grain initiation grows.

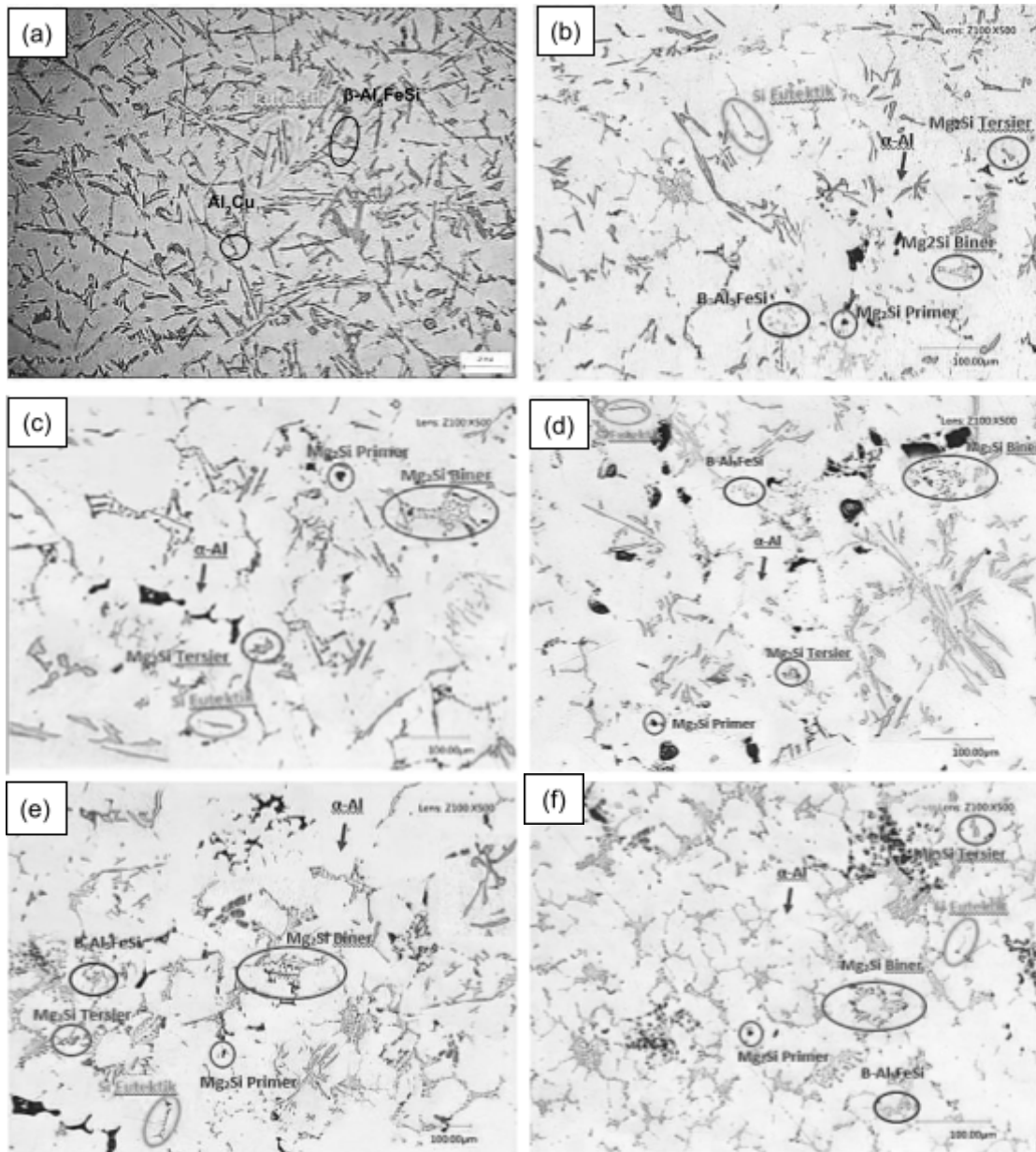


Figure 6. Microstructure observation by Optical Microscope (a) ADC12 alloy by magnification 200x [22], ADC12/nano- $Al_2O_3$  composites with addition of nano- $Al_2O_3$  particles by 500x magnification (b) 0.25 vf% (c) 0.3 vf% (d) 0.35 vf% (e) 0.4 vf% and (f) 0.5 vf%

EDS was performed on samples with an optimum amount of 0.35 vf% nano- $\text{Al}_2\text{O}_3$  addition % with a magnification of 300x carried out at 10 different points to observe spinel phase  $\text{MgAl}_2\text{O}_4$  and other intermetallic phases, as shown in figure 7 and result shown in table II.  $\text{Mg}_2\text{Si}$  phase is estimated to exist at points 012, 013, 014, and 015. Blocky morphology former point characterizes the primary  $\text{Mg}_2\text{Si}$  phase, while the remaining points have irregular fine-grained morphology. The indication for the  $\text{MgAl}_2\text{O}_4$  spinel phase is shown at point 016. The phase morphology at that point is not very clear, but there is a difference in color contrast with the matrix. The  $\text{MgAl}_2\text{O}_4$  phase will damage the oxide layer of  $\text{Al}_2\text{O}_3$  so that it will increase the contact between the reinforcing particles and the matrix. With a good bond between the matrix and the reinforcing particle, the transfer of charge from the matrix to the amplifier is getting better [27]. At points 011, 017, and 020, they contain ample Fe and lower magnesium which enables the formation of the intermetallic phase  $\text{Al}_5\text{FeSi}$  with a gray morphology and commonly in the form of faceted platelets.

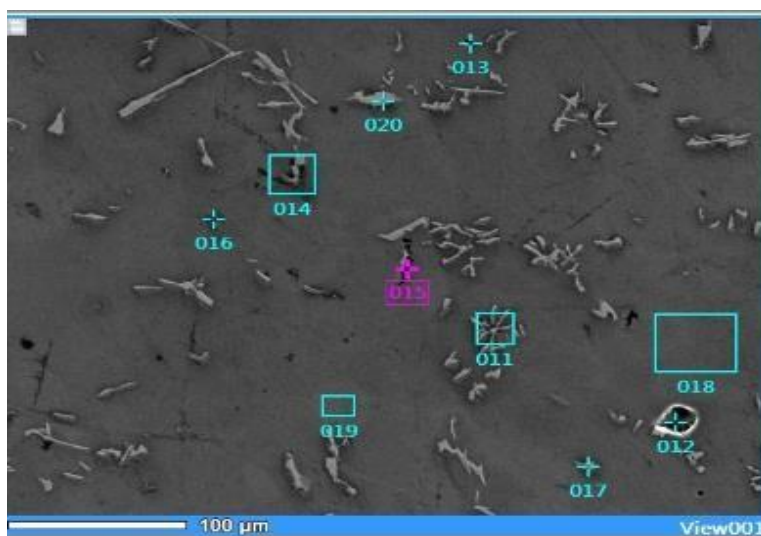


Figure 7. SEM observation on ADC12/Nano- $\text{Al}_2\text{O}_3$  composite with the addition 0.35 vf% nano- $\text{Al}_2\text{O}_3$  with magnification 150x. addition of nano- $\text{Al}_2\text{O}_3$  particles by 500x magnification (b) 0.25 vf% (c) 0.3 vf% (d) 0.35 vf% (e) 0.4 vf% and (f) 0.5 vf%

No.	Elements (wt%)						
	O	Mg	Al	Si	Ti	Fe	Cu
011	54.18	1,81	28,80	0,16		1,58	
012	55.64	2,43	25,93	0,17		0,06	
013	53.46	2,41	30,37	0,15		0,03	
014	53.92	2,34	29,65	0,13	0,01	0,82	
015	54.80	15,36	9,36	4,76		0,08	0,17
016	52.62	2,55	32,94	0,11			0,02
017	53.35	1,64	29,66	0,14		2,24	
018	53.20	2,70	31,74	0,12	0,01	0,03	
019	53.06	2,74	32,15	0,14	0,00	0,02	0,00
020	52.62	0,94	25,43	0,10		7,04	

Table II. EDS result corresponding SEM images in figure 7. on ADC12/nano- $\text{Al}_2\text{O}_3$  composite with the addition 0.35 vf% nano- $\text{Al}_2\text{O}_3$  with magnification 150X

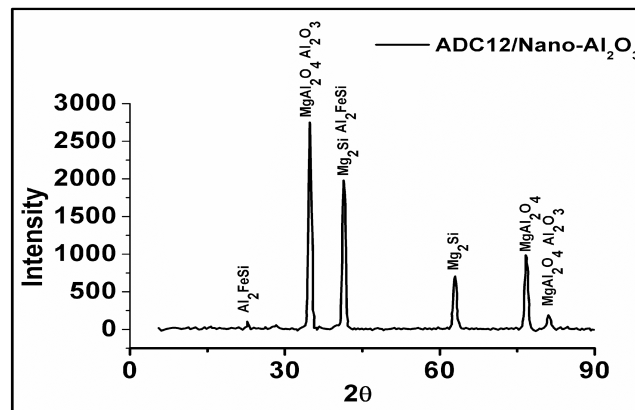


Figure 8. XRD spectra of ADC12/Nano-Al<sub>2</sub>O<sub>3</sub>

In detail, XRD was carried out to confirm that the MgAl<sub>2</sub>O<sub>4</sub> spinel phase emerges on ADC12/Nano-Al<sub>2</sub>O<sub>3</sub>. MgAl<sub>2</sub>O<sub>4</sub> and other phases that have been stated in table II, has proven formed as can be seen from figure 8.

#### IV. CONCLUSION

Addition of nano-Al<sub>2</sub>O<sub>3</sub> on ADC12 alloy has revealed remarkable mechanical properties of composites such as tensile strength and hardness. Correspondingly, the wear rate showing a promising result. Despite porosities and agglomeration have a critical role in reducing mechanical and tribological properties, spinel phase MgAl<sub>2</sub>O<sub>4</sub> perform its function properly. An optimum amount of nano-sized particle addition was determined in this study; thus, the spinel phase can cover all regions interface between matrix and nano-Al<sub>2</sub>O<sub>3</sub> particles. Furthermore, the addition of Al-5Ti-B and Sr has also enhanced the performance by reduced grain size and modified eutectic silicon form respectively. This study confirms that nano-Al<sub>2</sub>O<sub>3</sub> incorporated in ADC12 alloy with Al-5Ti-B, Al-Sr, and Mg addition generate high-performance materials and gives a constructive way ahead towards advanced material development.

#### V. ACKNOWLEDGMENT

Authors would like to thank The Directorate of Higher Education, Ministry of Higher Education and Research of Technology, Republic of Indonesia for financial support under Hibah PTUPT with contract number: NKB-1725/UN2.R3.1/HKP.05.00/2019.

#### REFERENCES

- [1]. S. A. Sajjadi, H. R. Ezatpour, and H. Beygi. 2011. "Microstructure and mechanical properties of Al–Al<sub>2</sub>O<sub>3</sub> micro and nano composites fabricated by stir casting". *Materials Science and Engineering: A*. volume. 528.
- [2]. C. Nie, H. Wang, and J. He. 2020. "Evaluation of the effect of adding carbon nanotubes on the effective mechanical properties of ceramic particulate aluminum matrix composites". *Mechanics of Materials*. volume. 142.
- [3]. P. Madhukar, N. Selvaraj, R. Gujjala, and C. S. P. Rao. 2019. "Production of high performance AA7150-1% SiC nanocomposite by novel fabrication process of ultrasonication assisted stir casting". *Ultrasonics Sonochemistry*. volume. 58.

- [4]. M. Karbalaee Akbari, H. R. Baharvandi, and O. Mirzaee. 2013. "Fabrication of nano-sized Al<sub>2</sub>O<sub>3</sub> reinforced casting aluminum composite focusing on preparation process of reinforcement powders and evaluation of its properties". *Composites Part B: Engineering*. volume. 55.
- [5]. M. Okayasu, Y. Ohkura, S. Takeuchi, S. Takasu, H. Ohfuji, and T. Shiraishi. 2012. "A study of the mechanical properties of an Al–Si–Cu alloy (ADC12) produced by various casting processes". *Materials Science and Engineering: A*. volume. 543.
- [6]. A. Razaghian, M. Emamy, A. A. Najimi, and S. H. S. Ebrahimi. 2009. "Sr effect on the microstructure and tensile properties of A357 aluminum alloy and Al<sub>2</sub>O<sub>3</sub>/SiC-A357 cast composites". *Materials Characterization*. volume. 60.
- [7]. R. Rana, R. Purohit, and S. Das. 2012. "Reviews on the influences of alloying elements on the microstructure and mechanical properties of aluminum alloys and aluminum alloy composites". *International Journal of Scientific and Research Publications*. volume. 2.
- [8]. B. Schultz, J. Ferguson, and P. Rohatgi. 2011. "Microstructure and hardness of Al<sub>2</sub>O<sub>3</sub> nanoparticle reinforced Al–Mg composites fabricated by reactive wetting and stir mixing". *Materials Science and Engineering: A*. volume. 530.
- [9]. A. Sangghaleh and M. Halali. 2008. "An investigation on the wetting of polycrystalline alumina by aluminium". *Journal of materials processing technology*. volume. 197.
- [10]. R. Lumley, T. Sercombe, and G. Schaffer. 1999. "Surface oxide and the role of magnesium during the sintering of aluminum". *Metallurgical and Materials Transactions A*. volume. 30.
- [11]. W. D. Callister and D. Rethwisch. 1994. "Materials Science and Engineering, John Willey & Sons". Inc., New York, USA.
- [12]. J. Garcia-Hinojosa and M. Surrupa. 2004. "Effect of grain refinement treatment on the microstructure of cast Al–7Si–SiCp composites". *Materials Science and Engineering: A*. volume. 386.
- [13]. S. Farahany, M. H. Idris, A. Ourdjini, F. Faris, and H. Ghandvar. 2015. "Evaluation of the effect of grain refiners on the solidification characteristics of an Sr-modified ADC12 die-casting alloy by cooling curve thermal analysis". *Journal of thermal analysis and calorimetry*. volume. 119.
- [14]. M. Gowrishankar, P. Hiremath, M. Shettar, S. Sharma, and S. Rao. 2020. "Experimental validity on the casting characteristics of stir cast aluminium composites". *Journal of Materials Research and Technology*.
- [15]. A. Mazahery and M. Ostadshabani. 2011. "Investigation on mechanical properties of nano-Al<sub>2</sub>O<sub>3</sub>-reinforced aluminum matrix composites". *Journal of composite materials*. volume. 45.
- [16]. L. F. Mondolfo. 2013. *Aluminum alloys: structure and properties*: Elsevier.
- [17]. Y.-T. Zhao, S.-L. Zhang, G. Chen, X.-N. Cheng, and C.-Q. Wang. 2008. "In situ (Al<sub>2</sub>O<sub>3</sub>+ Al<sub>3</sub>Zr) np/Al nanocomposites synthesized by magneto-chemical melt reaction". *Composites Science and Technology*. volume. 68.
- [18]. M. Dave and K. Kothari. 2013. "Composite material-aluminium silicon alloy: a review". *Paripex-Indian Journal Of Research*. volume. 2.
- [19]. T. Grøstad. 2014. "Nucleation of Primary Mg<sub>2</sub>Si in Al-Mg-Si Alloys." Thesis. Institutt for material teknologi.
- [20]. S. A. Sajjadi, M. T. Parizi, H. Ezatpour, and A. Sedghi. 2012. "Fabrication of A356 composite reinforced with micro and nano Al<sub>2</sub>O<sub>3</sub> particles by a developed compositing method and study of its properties". *Journal of alloys and compounds*. volume. 511.
- [21]. N. A. Belov, D. G. Eskin, and A. A. Aksenov. 2005. *Multicomponent phase diagrams: applications for commercial aluminum alloys*: Elsevier.
- [22]. A. Zulfia and L. T. Putriana. 2019. "Effect of strontium on the microstructure and mechanical properties of aluminium ADC12/Nano-SiC composite with Al-5TiB grain refiner by stir casting method". *Materials Research Express*. volume. 6.
- [23]. A. Handbook. 2004. "vol. 9: Metallography and Microstructures". Ed. GF Van der Voort, ASM International, New York.

- 
- [24]. K. M. Shorowordi, T. Laoui, A. A. Haseeb, J.-P. Celis, and L. Froyen. 2003. "Microstructure and interface characteristics of B<sub>4</sub>C, SiC and Al<sub>2</sub>O<sub>3</sub> reinforced Al matrix composites: a comparative study". *Journal of Materials Processing Technology*. volume. 142.
- [25]. M. Tebib, A. Samuel, F. Ajersch, and X.-G. Chen. 2014. "Effect of P and Sr additions on the microstructure of hypereutectic Al–15Si–14Mg–4Cu alloy". *Materials Characterization*. volume. 89.
- [26]. Y. Mingbo and S. Jia. 2009. "Modification and refinement mechanism of Mg<sub>2</sub>Si phase in Sr-containing AZ61-0.7 Si magnesium alloy". *China Foundry*. volume. 6.
- [27]. S. Mohan, G. Gautam, N. Kumar, R. K. Gautam, A. Mohan, and A. K. Jaiswal. 2016. "Dry sliding wear behavior of Al-SiO<sub>2</sub> composites". *Composite Interfaces*. volume. 23.